Chemistry & Biology, Vol. 9, 897–906, August, 2002, ©2002 Elsevier Science Ltd. All rights reserved. PII S1074-5521(02)00191-6

Functional Analysis of the Lipoglycodepsipeptide Antibiotic Ramoplanin

Predrag Cudic,[1] Douglas C. Behenna,[1] James K. Kranz,[1] Ryan G. Kruger,[1] A. Joshua Wand,[1] Yuri I. Veklich,[2] John W. Weisel,[2] and Dewey G. McCafferty[1,3]

[1]Johnson Research Foundation
Department of Biochemistry and Biophysics and
[2]Department of Cell and Developmental Biology
The University of Pennsylvania School of Medicine
Philadelphia, Pennsylvania 19104

Summary

The peptide antibiotic ramoplanin is highly effective against several drug-resistant gram-positive bacteria, including vancomycin-resistant *Enterococcus faecium* (VRE) and methicillin-resistant *Staphylococcus aureus* (MRSA), two important opportunistic human pathogens. Ramoplanin inhibits bacterial peptidoglycan (PG) biosynthesis by binding to Lipid intermediates I and II at a location different than the *N*-acyl-D-Ala-D-Ala dipeptide site targeted by vancomycin. Lipid I/II capture physically occludes these substrates from proper utilization by the late-stage PG biosynthesis enzymes MurG and the transglycosylases. Key structural features of ramoplanin responsible for antibiotic activity and PG molecular recognition have been discovered by antibiotic semisynthetic modification in conjunction with NMR analyses. These results help define a minimalist ramoplanin pharmacophore and introduce the possibility of generating ramoplanin-derived peptide or peptidomimetic antibiotics for use against VRE, MRSA, and related pathogens.

Introduction

The widespread use of broad-spectrum antibiotics has placed enormous selective pressures on bacterial populations, forcing the evolution of resistance mechanisms [1, 2]. Antibiotic resistance results in morbidity and mortality from treatment failures and increased health care costs [3]. The lipoglycodepsipeptide antibiotic ramoplanin factor A2 (**1**, Figure 1) is a promising candidate for treatment of antibiotic-resistant gram-positive infections. Produced by *Actinoplanes* ATCC 33076, ramoplanin is highly active against numerous gram-positive bacteria, including MRSA [4–8], VRE, and those resistant to ampicillin and erythromycin [8–13]. It is currently in phase III clinical trials in the United States for the suppression of VRE in the gastrointestinal tract and for prevention of bloodstream infections caused by VRE. To date, no cases of clinical or laboratory-generated resistance to the antibiotic have been reported [14, 15].

Ramoplanin does not target an enzyme directly, but rather sequesters the substrates of PG biosynthesis enzymes. In a similar manner as the glycopeptides and select lantibiotics (nisin, epidermin, mersacidin, and actagardine), ramoplanin captures Lipid I and II. Sequestration of Lipid I/II by ramoplanin precludes their normal utilization as substrates by MurG and the transglycosylase (TGase) enzymes. As a result, bacteria produce a mechanically weakened cell wall. In the presence of soluble analogs of Lipid intermediates, we [16] and Walker [17] have demonstrated that ramoplanin undergoes a ligand-induced aggregation resulting in the formation of insoluble fibrils. Solublization of the fibrils with 20% dimethylsulfoxide (DMSO) facilitated determination of dissociation constants and identification of the binding interface with PG monomers by NMR [16]. It was shown that the majority of chemical shift changes and intermolecular NOEs in the complex were localized between the muramyl carbohydrate and adjacent pyrophosphate of the PG monomer and the Hpg^3-Orn^{10} stretch of ramoplanin (Figure 1). This octapeptide stretch is also conserved among the primary sequences of enduracidins A and B [18–20] and likely is found in janiemycin [21–23], cell-wall-active peptide antibiotics that are predicted to possess Lipid I/II binding activity [16]. Furthermore, ramoplanin's overall fold is shared by two lantibiotics, mersacidin [24–27] and actagardine [28], strongly suggesting that all three antibiotics are functionally related [16, 28–32].

In this report, we take steps toward reducing the complex structure of ramoplanin to its minimalist bioactive pharmacophore. Here, we dissect the contribution of functional groups within the ramoplanin sequence and assess their effects on its antimicrobial activity, its ability to bind bacterial PG biosynthesis monomers and related synthetic analogs (Figure 2), and to form fibrils via self-association of the antibiotic-PG monomer complex. Defining the minimal structural requirements responsible for ramoplanin's antimicrobial activity will help facilitate chemical synthesis of the antibiotic by reducing structural complexity and will also promote judicious chemical modification for structure/activity analyses and modulation of biological or physiochemical properties. The information gained from these studies will help guide the design of ramoplanin-derived anti-VRE or anti-MRSA antibiotics.

Results and Discussion

Ramoplanin and Enduracidin Are Structurally and Functionally Related

Previously, we used NMR methods combined with chemical synthesis to isolate the minimal region of PG capable of associating with ramoplanin and to determine the structure of the ramoplanin-PG intermediate binding interface [16]. It was determined that residues Hpg^3-Orn^{10} of ramoplanin participated in binding PG biosynthetic intermediates (Figure 1). In this study, we turn our attention to investigating the structural basis for ramoplanin's biological activity in hopes of defining a minimal bioactive pharmacophore and to further dissect

[3]Correspondence: deweym@mail.med.upenn.edu

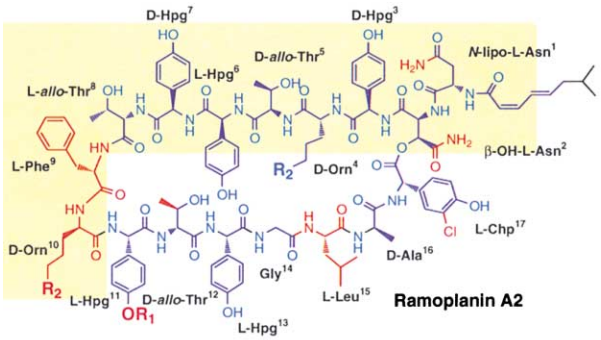

	R_1	R_2
1	α-D-Mannosyl-(1→2)-α-D-mannose	NH_3^+
2	H	NH_3^+
3	α-D-Mannosyl-(1→2)-α-D-mannose	$HNC(NH)NH_3^+$
4	α-D-Mannosyl-(1→2)-α-D-mannose	$HN^+(CH_2)_2CH(CH_3)_2$
5	α-D-Mannosyl-(1→2)-α-D-mannose	NHAc
6	α-D-Mannosyl-(1→2)-α-D-mannose	NH_3^+ (Lactone hydrolyzed)

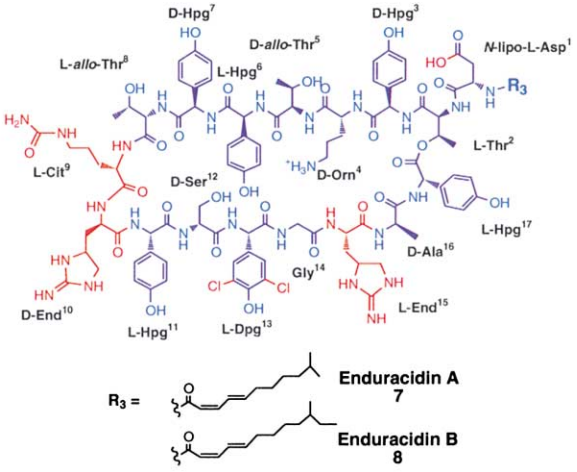

Figure 1. Chemical Structures of the Antibiotic Ramoplanin Factor A2 from *Actinoplanes* ATCC 33076, the Semisynthetic Ramoplanin Analogs Prepared in This Study, and the Structurally Related Enduracidin Antibiotics from *Streptomyces fungicidicus* B5477

Common structural elements of the sequences of ramoplanin and enduracidins are colored blue. Divergent structural elements are colored red. Highlighted in yellow are the amino acid residues that exhibit marked NMR chemical shift changes upon binding PG precursors [16]. A similar sequence is found in the enduracidins. Nonstandard residues are denoted as follows: Chp, 3-chloro-4-hydroxyphenylglycine; Cit, citrulline; Dpg, 3,5-dichloro-4-hydroxyphenylglycine; End, enduracididine; Hpg, 4-hydroxyphenylglycine.

the sequence requirements responsible for high affinity PG biosynthetic intermediate recognition and antibiotic activity.

A substructure search of the Hpg[3]-Orn[10] sequence in known peptide antibiotics yielded the enduracidin family of cell-wall-active lipodepsipeptide antibiotics produced by *Streptomyces fungicidicus* B5477 [19]. Highly homologous to ramoplanin, the enduracidins contain the sequence *allo*-Thr[8]-D-Hpg[7]-Hpg[6]-D-*allo*-Thr[5]-D-Orn[4]-D-Hpg[3], which exhibits sequence similarity to ramoplanin's Hpg[3]-Orn[10] PG recognition sequence (Figure 1) [18]. In the enduracidins, the amino acids enduracididine (End[10]) and citrulline (Cit[9]) are found in positions corresponding to the Orn[10] and Phe[9] residues of ramoplanin. The similarity of the PG recognition sequences of the two antibiotics strongly suggests that they possess similar mechanisms of action.

To test this hypothesis, we examined enduracidin for its ability to bind to citronellyl-Lipid I (**10**), a soluble derivative of the PG biosynthesis intermediate Lipid I [33], and to self-associate following complexation. Since similar behavior has been observed for ramoplanin with compound **10**, aggregate formation (e.g., fibril formation for ramoplanin) serves as a convenient predictor of PG complexation [16]. Indeed, upon mixing equimolar homogeneous solutions of enduracidin (1 mM, 4% DMSO) with **10** (1 mM), an amorphous precipitate formed immediately (Figure 3). MS analysis of the precipitate showed that it contained both enduracidin and **10**. Similar aggregates were obtained by mixing enduracidin solutions

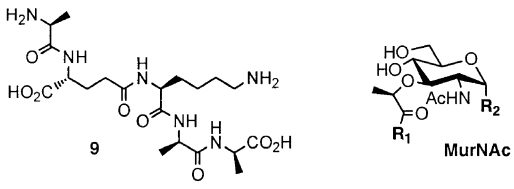

	R_1	R_2
10	L-Ala-D-γ-Glu-L-Lys-D-Ala-D-Ala-OH	
11	L-Ala-D-γ-Glu-L-Dap-D-Ala-D-Ala-OH	UDP
12	L-Ala-D-γ-Glu-L-Dap-OH	UDP
13	L-Ala-D-γ-Glu-L-Dap-OH	OPO_3^{2-}
14	OH	
15	L-Ala-D-γ-Gln	OH

Figure 2. Chemical Structures of Synthetic and Naturally Occurring Analogs of Bacterial Peptidoglycan Monomers Used in This Study

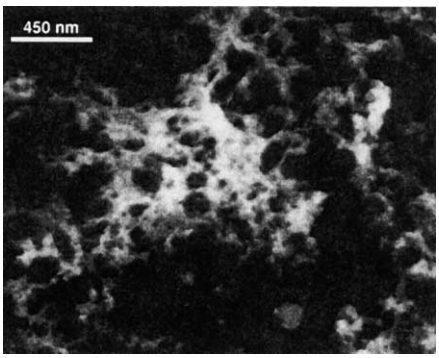

Figure 3. Transmission Electron Micrograph of the Aggregate Formed from the Complexation of Enduracidin with Compound 10

with solutions of compounds **11** or **12**. Due to the low solubility of enduracidin in aqueous solutions, DMSO was added to facilitate its dissolution; thus a final concentration of 2% DMSO was present in the complexation assay. We have previously shown that addition of DMSO reduces or altogether eliminates fibril formation during complexation of ramoplanin with compounds **11** or **12** [16]. Since an amorphous aggregate formed instead of an ordered fibril as was observed for ramoplanin, it is likely that the presence of 2% DMSO required to solublize enduracidin was of sufficient concentration to compete for intercomplex hydrogen bonding and/or π-π interactions that might have been critical for the formation and coalescence of protofibrils or aggregates into ordered fibrils. The limited solubility of enduracidin in water might also play a role in altering the morphology of the precipitate. Nevertheless, these observations are strongly suggestive of the existence of a common mechanism of action for both ramoplanin and enduracidin.

Structural Comparison of Enduracidin to Ramoplanin Suggests the Existence of a Common Antibiotic Pharmacophore

Enduracidin and ramoplanin share a number of structural similarities that point to a common bioactive antibiotic pharmacophore (Figure 1). Both are 17-residue lipodepsipeptides. Both are *N*-acylated with *cis*,*trans* fatty acids, although the acyl chains in enduracidins A and B are considerably longer than that of ramoplanin factor A2, and correspondingly these antibiotics are less soluble than ramoplanin in water. However, unsaturation of this acyl appendage appears to be unimportant, for Ciabatti and coworkers previously showed that catalytic hydrogenation of ramoplanin to afford the fully saturated *N*-acyl tail did not alter its antibiotic activity [34].

Both antibiotics appear to require chlorinated hydroxyphenylglycine residues. In ramoplanin, a monochlorinated hydroxyphenylglycine is found in position 17. This residue is one of the three aryl groups comprising the Chp^{17}-Hpg^{3}-Phe^{9} hydrophobic core. In the NMR structure of ramoplanin [35], the chlorine of Chp^{17} appears to serve a stabilizing role, as it is buried deep within this hydrophobic core. Similarly, enduracidins contain a dichlorinated hydroxyphenylglycine in position 13 (Dpg^{13}) (Figure 1). Ramoplanin residue 13 lies juxtaposed across the β sheet from Chp^{17}, so it is possible that Dpg^{13} might function in a similar manner as Chp^{17} to stabilize the conformation of enduracidins. Similar chlorinated aryl groups are found in complestatin, the chloropeptins, kistamycin, and the glycopeptide antibiotic vancomycin. In the case of the latter, removal of the chlorines alters its antimicrobial activity [36, 37]. It remains to be determined if chlorination is important for the antimicrobial activity of ramoplanin or the enduracidins.

Ramoplanin contains a lactone formed between the α-carboxylate of Chp^{17} and the 3-hydroxyl of β-OH-Asn^{2}. The enduracidins contain a structurally less complex lactone linkage between the α-carboxylate of Hpg^{17} and the side chain hydroxyl of Thr^{2} (Figure 1). As will be detailed below, the significantly reduced antibiotic activity of linearized ramoplanin suggests that the lactone is an important structural component. These observations are also consistent with possible participation of residues upstream of Hpg^{3} (e.g., Asn^{1}, Asn^{2}, or Chp^{17}) in binding Lipid I/II or stabilizing the bioactive conformation and, taken together with the functional parallels between ramopanin and enduracidin, strongly suggest the existence of a common bioactive pharmacophore.

Glycosylation Confers Both Conformational Stability and Protection from Acid Hydrolysis to Ramoplanin

We wished to establish whether the mannose disaccharide group at position Hpg^{11} influenced Lipid I/II binding. Ciabatti and coworkers demonstrated that this carbohydrate could be hydrolyzed by treatment with trimethylsilyl iodide [38, 39]. The resulting aglycon possesses antimicrobial activity comparable to the parent antibiotic, suggesting that this structural element is not essential for antimicrobial activity [38, 39]. The enduracidins are not glycosylated, yet both ramoplanin and enduracidin similarly bind PG biosynthesis monomers in vitro and exhibit potent antimicrobial activity in vivo. We prepared ramoplanin aglycon (**2**), purified it to homogeneity by HPLC, and confirmed Ciabatti's observation of equivalent antimicrobial activity as the parent antibiotic against a *B. subtilis* gram-positive bacterial test strain (MIC = 0.03 μg/ml for both antibiotics) [38, 39]. As predicted, titration of a solution of **2** (1.0 mM) against PG monomer analogs citronellyl-Lipid I (**10**) [33, 40], Park's nucleotide (**11**) [41], and UDP-MurNAc-tripeptide (**12**) resulted in the formation of insoluble fibrils (Figure 4). As depicted in Table 1, ^{1}H NMR titration experiments conducted in DMSO/D_2O (20:80, v/v), a solvent mixture capable of greatly minimizing fibril formation, facilitated the determination of dissociation constants (K_d) for the antibiotic-ligand complex. The complex was in fast exchange with its dissociated components on the NMR chemical shift timescale [16]. The combination of residual fibril formation and NMR spectral overlap between the citronellyl methyls and lactyl ether methyls of **10** limits the accuracy of the determined K_d to a simple upper boundary estimate of $\leq$200 μM. Similar measurements indicate that aglycon **2** has a $\sim$2-fold lower affinity for Park's nucleotide **11** (K_d = 330 $\pm$ 30 μM) when compared to ramoplanin (K_d = 180 $\pm$ 20 μM), but an almost 2-fold increased affinity for compound **12** (K_d = 1300 $\pm$ 30 μM versus K_d = 2380 $\pm$ 30 μM). Glycosylation of ramoplanin therefore imparts no influence on antimicrobial activity and only has a slight influence on the energetics of PG monomer binding.

Removal of the disaccharide both increased conformational flexibility and susceptibility of the aglycon to acid hydrolysis. Comparison of the 2D NMR NOESY spectra of ramoplanin with aglycon **2** showed that the aglycon exists in multiple conformations in solution, but the parent compound **1** exists in a single conformation on the NMR timescale (data not shown). Since glycosylation can confer conformational stability to proteins and peptides [42], it is believed that ramoplanin's mannosyl disaccharide helps stabilize the β sheet conformation.

During preparative purification of aglycon **2** by HPLC, we observed the time-dependent decomposition of the

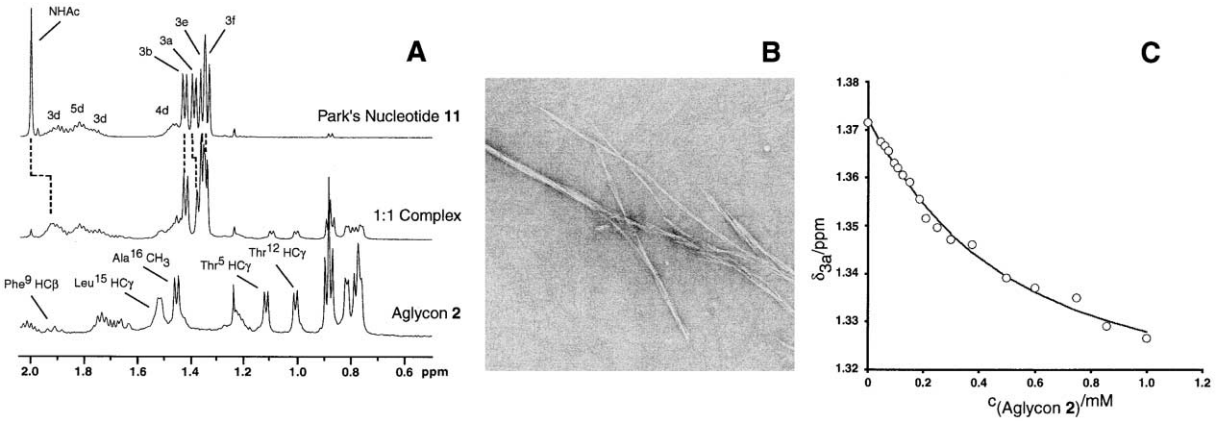

Figure 4. NMR Analysis of Peptidoglycan Biosynthesis Intermediate Complexation by Ramoplanin Aglycon (2)

(A) Part of the aliphatic region of the ^{1}H NMR spectrum of free ramoplanin aglycon (**2**), free Park's nucleotide (**11**), and a 1:1 mixture of the two illustrating the chemical shift changes that occur upon binding.

(B) Representative transmision electron micrograph of the fibrils formed from the complexation of aglycon **2** with Park's nucleotide (**11**). Fibrils formed from the interaction of ramoplanin (**1**) or its derivatives **2–4** with citronellyl-Lipid I (**10**) and Park's nucleotide (**11**), respectively, exhibited similar morphology.

(C) Representative K_d determination plot of the binding of ramoplanin aglycon (**2**) to Park's nucleotide (**11**) as obtained by ^{1}H NMR titration. The curve denotes the experimental (open circles) and calculated (solid line) chemical shifts (δ) of the lactyl ether methyl protons (3a) of **11** as a function of ramoplanin concentration.

antibiotic in acidic solutions. Although decomposition is rapid in neat trifluoroactic acid, modest rates of decomposition occurred in 0.1% aqueous TFA and during exposure to solutions containing 1%–10% HCl or AcOH. In contrast, the parent antibiotic was completely resistant to acid hydrolysis over the same time regimes and conditions examined. It is likely that ramoplanin glycosylation reflects an evolutionary adaptation by its *Actinoplanes* producer for ensuring antibiotic integrity in low-pH extracellular environments, for antibiotic protection from deleterious proteolytic degradation, or for producer immunity. Collectively, these studies confirm that dimannosylation of Hpg^{11} does not influence ramoplanin's antibiotic activity but likely serves to protect the antibiotic from deleterious hydrolysis.

Intriguingly, unlike glycopeptide and macrolide antibiotics, specific genes encoding glycosyltransferases are not found within the ramoplanin biosynthetic gene locus [43]. Glycosylation therefore likely occurs after nonribosomal peptide assembly by glycosyltransferases involved with other primary or secondary metabolism processes. Although the biosynthetic locus for enduracidin has not yet been identified and sequenced, *Streptomyces fungicidicus* B5477 apparently has not evolved or does not employ glycosylation as a protective measure, perhaps because the antibiotic is perfectly stable in the environment to which it is released or because primary structural differences between ramoplanin and enduracidin are sufficient to confer peptide stability. Enduracidin, like ramoplanin, is known to be highly stable in acidic solutions [44].

Since aglycon **2** contains the full complement of wild-type ramoplanin's antimicrobial activity, removal of the mannosyl disaccharide from **1** leads to a bioactive pharmacophore with significantly reduced chemical complexity. Boger and coworkers have recently described

Table 1. Fibril Formation and Dissociation Constants of Ramoplanin and Related Analogs with Peptidoglycan Precursors and Related Fragments

Peptidoglycan Analogs	Ramoplanin Analogs					
	1	2	3	4	5	6
	Fibril Formation (Yes/No, Conditions), Dissociation Constant (μM)					
10	Y(A), Y(B) p.p.	Y(A), Y(B) p.p.	N(A), N(B) n.d.	N(A), N(B) n.d.	N(A), N(B) n.d.	N(A), N(B) n.i.
11	Y(A), N(B) 180 ± 20	Y(A), N(B) 330 ± 50	Y(A), N(B) 170 ± 30	Y(A), N(B) 130 ± 20	Y(A), N(B) 1340 ± 320	N(A), N(B) n.i.
12	Y(A), N(B) 2380 ± 440	Y(A), N(B) 1300 ± 230	Y(A), Y(B) n.d.	Y(A), N(B) 1280 ± 140	Y(A), N(B) n.i.	N(A), N(B) n.i.

Conditions for complexation and fibril formation: [ramoplanins] = 1.0 mM, [peptidoglycan fragments/analogs] = 1.0 mM in either (A) D_2O (pH 7.0) or (B) 20% DMSO/D_2O (pH 7.0). Dissociation constants were determined by ^{1}H NMR titration at 600 MHz in 20% DMSO-$_{d6}$/D_2O (pH 7.0). n.i., no appreciable interaction, i.e., a homogeneous solution with no antibiotic-peptidoglycan precursor binding was observed or $K_d > 10$ mM as determined by ^{1}H NMR; p.p., partial precipitation precluded accurate K_d determination; n.d., not determined. Peptidoglycan fragments **13–15** failed to associate with derivatives **1–6** under these conditions.

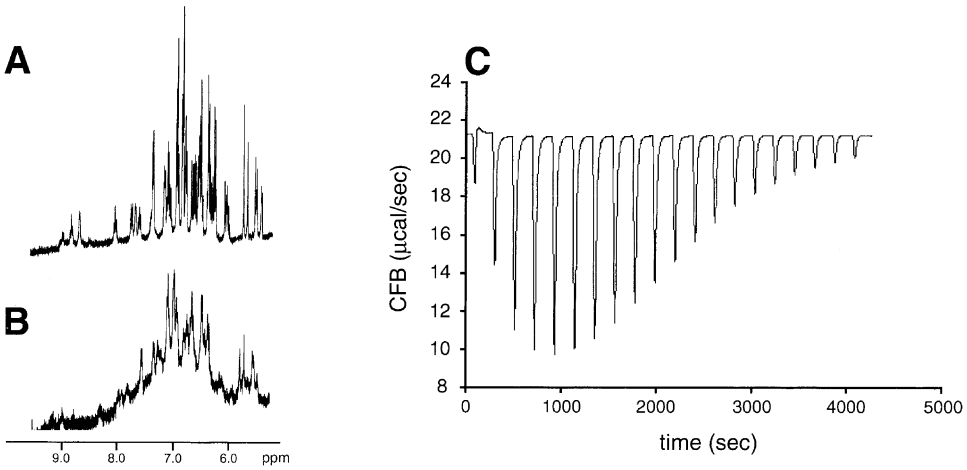

Figure 5. Interaction of [Orn^4,Orn^{10}]-Diguanidylated Ramoplanin with Park's Nucleotide

(A) Aromatic and amide region of the ^{1}H NMR spectrum of free [Orn^4,Orn^{10}]-diguanidylated ramoplanin (**3**). The spectrum was obtained at 500 MHz at 25°C in D_2O (pH 6.0).

(B) The same aromatic and amide region of the ^{1}H NMR spectrum of [Orn^4,Orn^{10}]-diguanidylated ramoplanin (**3**) with equimolar Park's nucleotide (**11**) depicting the line broadening and chemical shift changes that occur upon binding.

(C) Isothermal titration calorimetry data from the titration of [Orn^4,Orn^{10}]-diguanidylated ramoplanin (**3**) with compound **11**. The complex pattern of heat released during the titration is indicative of ligand-induced aggregation [46, 47].

an elegant total synthesis of the aglycon of ramoplanin A2 and ramoplanose by solution-phase methods [45]. Avoidance of construction of ramoplanin's dimannosyl carbohydrate will certainly facilitate the chemical assembly of analogs for structure/activity studies.

Ramoplanin Ornithines 4 and 10 Participate in Capture of Peptidoglycan Lipid Intermediates

Previously, we determined that ramoplanin residues Hpg^3-Orn^{10} are involved in the capture of PG intermediates [16]. Ornithines 4 and 10 are the only charged residues in the ramoplanin sequence and thus are candidates for interacting with the anionic Lipid I/II pyrophosphate and/or peptidyl carboxylates. To examine the contribution of individual ramoplanin functional groups in the recognition of PG monomers, several semisynthetic modifications were performed on the antibiotic, and their antimicrobial and PG binding properties were assessed. Orn residues were converted to guanidine, secondary amine, and acetamide functional groups, purified, and assessed for antimicrobial activity and for the ability to bind to PG intermediates and/or to form fibrils (Table 1).

Treatment of ramoplanin (**1**) with 1*H*-pyrazole-1-carboxamidine provided the [Orn^4,Orn^{10}]-diguanidylated derivative **3** that possessed a MIC of 0.25 μg/ml, a value approximately 8-fold higher than the wild-type antibiotic. NMR analysis of ramoplanin derivative **3** with PG precursors **11** or **12** in D_2O showed clear evidence of complexation and formation of a large, soluble aggregate (Figure 5). Results from isothermal titration calorimetry experiments conducted with **3** and **11** also clearly indicated that a ligand-induced aggregation occurred during the titration (Figure 5) [46, 47]. Insoluble fibrils could be produced from soluble fibril preparations by increasing the ionic strength to ≥100 mM. Fibrils formed under these high ionic strength conditions exhibited similar morphology to those formed by ramoplanin (**1**) or aglycon **2**. In 20% DMSO, the K_d of ramoplanin derivative **3** with PG precursor **11** was nearly identical to that of wild-type **1** (170 ± 30 μM); however, soluble fibril formation during the NMR titration precluded K_d determination with **12** (Table 1).

[Orn^4,Orn^{10}]-Diisovaleryl ramoplanin (**4**), prepared by reductive alkylation with isovaleryl aldehyde and $NaCNBH_3$, maintains the side chain amine cationic charge but contains increased steric bulk about the ornithine sidechain amine. This compound shows a significantly reduced MIC (4 μg/ml; 133-fold lower than wild-type), yet the dissociation constants of **4** with compounds **11** and **12** were slightly lower than wild-type (130 ± 20 μM and 1280 ± 140 μM, respectively) (Table 1).

Finally, removal of the cationic charge by [Orn^4, Orn^{10}]-diacetylation produced derivative **5**. This compound exhibited both a markedly reduced antibiotic activity (MIC = 16 μg/ml; 533-fold lower than ramoplanin) and almost a 10-fold decrease in binding affinity with **11** (K_d = 1340 ± 320 μM) (Table 1). Furthermore, it failed to show detectable binding to **12**. The strong correlation between the presence of cationic charges on the Orn^4, Orn^{10} γ-amino groups and the affinity of the antibiotic toward PG precursors **11** and **12** support the hypothesis that these residues anchor the PG ligand in the proper orientation for binding using electrostatic or hydrogen bonding interactions [16]. Preservation of charge on these residues is also essential for antimicrobial activity, with the general order of activity of 1° amine > guanidine > 2° amine for those analogs tested.

Although enduracidins contain only one ornithine (Orn^4), they do, however, contain two cationic guanidine-like enduracididine residues in position 10 (End^{10}) and in position 15 (End^{15}) (Figure 1). It is likely that End^{10} functions in a similar manner as Orn^{10} of ramoplanin. These results suggest that ramoplanin positions 4 and/or 10 are able to tolerate a number of diverse substitu-

tions, providing they maintain a positive charge at these sites.

Ramoplanin Employs a Conformationally Constrained Recognition Sequence for Capture of Lipid Intermediates

To determine if the Hpg^3-Orn^{10} ramoplanin sequence and flanking residues were capable of sequestering peptidogycan derivatives when presented in the form of a linear peptide instead of the wild-type conformationally constrained lactone, we converted ramoplanin (**1**) into its linear form (**6**) by hydrolysis with 1% triethylamine/water [48] and tested its ability to bind PG analogs by NMR. Williams and coworkers previously demonstrated that the hydrolyzed linear form of the closely related antibiotic ramoplanose maintained significant native-like β sheet structure in D_2O after hydrolysis [48]. We found that linearized ramoplanin possessed a MIC value of 64 μg/ml, a 2133-fold increase from that of the wild-type antibiotic (0.03 μg/ml). Thus, almost all of the antibiotic activity was lost when the lactone was hydrolyzed. Compound **6** did not bind citronellyl-Lipid I (**10**) nor related compounds **9** or **11–15** (Table 1). This data suggests that high-affinity capture of PG monomers requires presentation of residues along the Hpg^3-Orn^{10} sequence in a specific three-dimensional conformation. Presentation in its bioactive conformation is facilitated by the constraining Asn^2-Chp^{17} lactone. These data also suggest that important interactions not previously identified by NMR analysis in 20% DMSO are present only when the lactone is intact.

To confirm that residues along the Hpg^3-Orn^{10} stretch of ramoplanin were necessary and sufficient for PG complexation, we designed and synthesized the cyclic peptide N^{α}-octanoyl-Asn-Asn-*cyclo*[Cys-D-Orn-Phe-*allo*Thr-D-Hpg-D-*allo*Thr-Hpg-Cys]-D-Orn-NH_2 (**16**, Figure 6), a conformationally constrained mimic of the Hpg^3-Orn^{10} ramoplanin PG recognition sequence, and examined its propensity to bind Park's nucleotide (**11**) by NMR. Peptide **16** was synthesized by standard Fmoc solid-phase peptide synthesis methods and cyclized to the disulfide by air oxidation in 20% DMSO (pH 8.0). Two cysteine residues were placed in the sequence as replacements for Hpg^3 and Phe^9 in order to constrain the peptide into conformational subpopulations that orient Asn^2 near Thr^8, as is observed in the NMR structure of ramoplanin (Figure 6) [35]. In addition, ramoplanin's *N*-acyl *cis,trans* 7-methyl-2,4-octadieneoic fatty acid was replaced by a commercially available isosteric octanoic acid.

To determine if peptide **16** was capable of binding PG monomers, we conducted an NMR titration of reduced and oxidized **16** (0.5 mM) with Park's nucleotide in D_2O (pH 6) (Figure 6). Dithiothreitol-reduced **16** did not interact with compound **11**. However, we did observe a specific interaction with the oxidized form of **16** and **11**. The NMR spectrum of disulfide-linked **16** with **11** revealed marked chemical shift changes indicative of complexation, although no fibrils formed by visual inspection or by electron microscopy analysis (Figure 6). The magnitude of these chemical shift changes resembled those observed for ramoplanin with **11**; however, due to the cooperative behavior of the complexation, a true K_d value was not assigned but is estimated to be ~1 mM (Figure 6). The NMR chemical shift data indicated that peptide **16** binds to the terminal D-Ala-D-Ala dipeptide of **11** under these concentrations. Ramoplanin binds primarily to the muramyl carbohydrate and adjacent L-Ala residue of PG precursors, but significant contacts are made to the pentapeptide terminus. In fact, deletion of the last two D-Ala residues reduces binding affinity on average by 10-fold [16]. In this conformationally constrained peptide, we have dissected out a subset of ramoplanin's binding interface with **11**. Although the observed interaction is clearly distinct and specific for the pentapeptide terminus of **11**, peptide **16** was devoid of antimicrobial activity to >512 μg/ml, suggesting that antimicrobial activity requires additional residues or is supported by an alternate receptor conformation which might have been disallowed by the design of **16**.

Although ramoplanin derivative **16** bound Park's nucleotide with modest affinity, it neither possessed antimicrobial activity nor formed fibrils following ligand capture. This interesting observation raises the question as to what, if any, physiological role antibiotic oligomerization or intermolecular complex association (i.e., fibril formation) might play in the bacterial killing mechanism. Previously, we provided evidence of a ligand-induced conformational change in ramoplanin that results in the flattening of its cup-shaped architecture when liganded [16]. Following complexation, the Chp^{17}-Hpg^3-Phe^9 hydrophobic core becomes exposed to bulk solvent, creating a potential surface for intermolecular aggregation [16]. It has not yet been established if ramoplanin-PG Lipid intermediate complexes polymerize in a membrane environment as they do in free solution. Once liganded, the conformational changes observed by ramoplanin in solution and concomitant intercomplex aggregation certainly raise the possibility that oligomerization could occur at the level of the membrane, where it would be expected to impart beneficial effects, such as improved capture of both PG monomers and actively polymerizing PG chains.

Conclusion: Toward a Minimalist Ramoplanin

In this study, we take steps toward further elucidating the molecular basis of ramoplanin's complex mechanism of action and defining a minimal bioactive pharmacophore. These structure/activity experiments, taken together with comparative analysis of the structure and function of ramoplanin and the enduracidins, imply that a minimal functional pharmacophore exists that unites the two antibiotic classes. Ciabatti and coworkers previously established that both glycosylation and *N*-acyl lipid unsaturation were not required for conferring high-level antimicrobial activity [34, 39]. Our structure/function studies with ramoplanin highlight the significance of Hpg^{11} mannosylation in instilling conformational stability and resistance to degradation, the consequence of disrupting the Chp^{17}-Asn^2 lactone bond on antimicrobial activity, the requirement for cationic charge on ramoplanin's two ornithines, and the importance of presentation of the Hpg^3-Orn^{10} PG binding sequence in a conformationally restrained manner. Since similar structural features are echoed by the enduracidins, one can assume that many of these sequence and structural elements may be functionally interchangeable between the two antibiotic

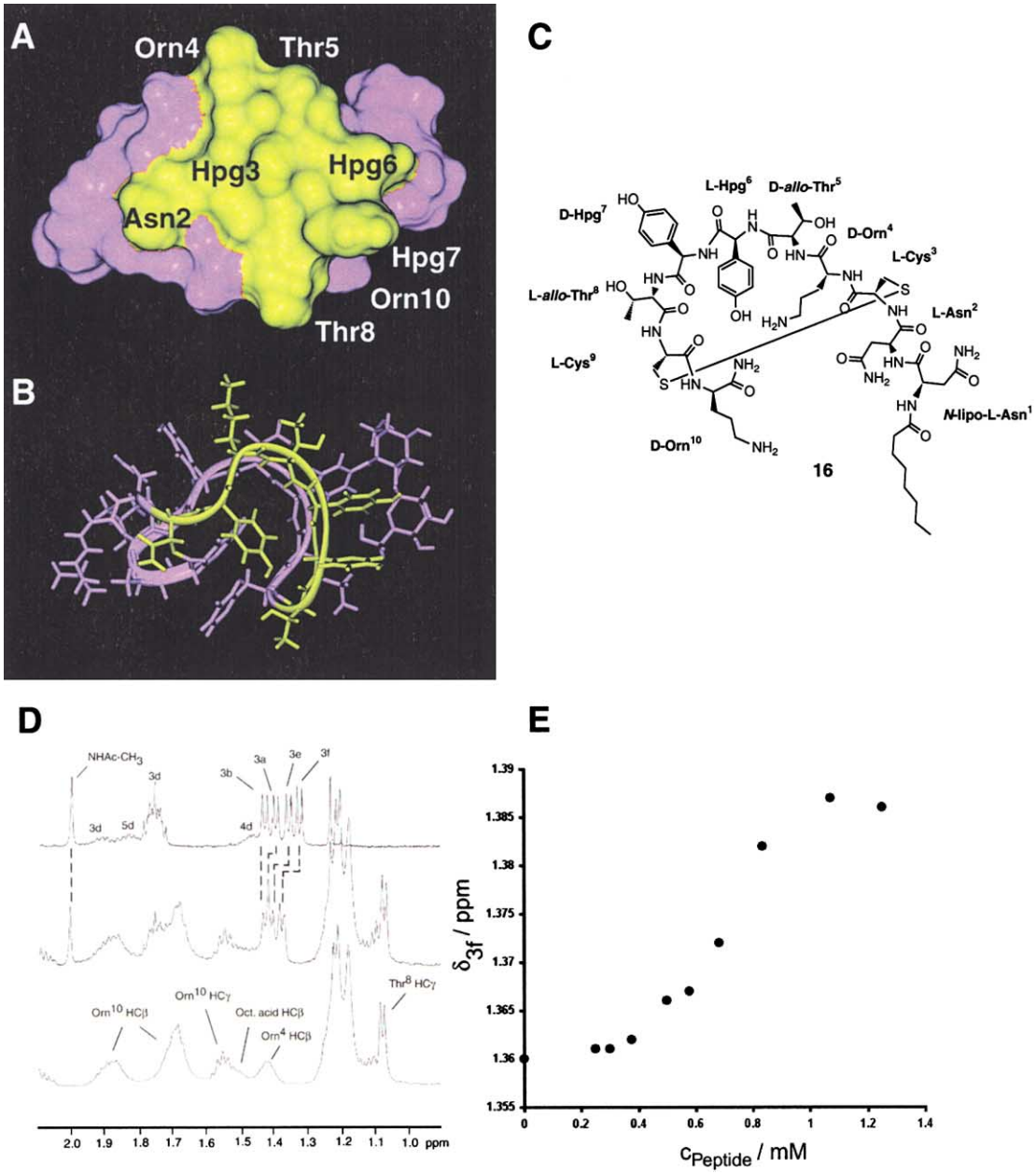

Figure 6. Design and Biophysical Analysis of a Ramoplanin-Derived Cyclic Peptide that Binds a Peptidoglycan Biosynthesis Intermediate

(A) Surface representation of ramoplanin (**1**) based on the NMR solution structure obtained in 20% DMSO [35]. Residues participating in capture of peptidoglycan monomer/lipid intermediates identified by NMR analysis are colored in yellow and lie on one face of the antibiotic surface.

(B) Stick representation of the structure of ramoplanin showing that the residues comprising the binding interface lie along one of the two β strands eminating from the Thr^8-Phe^9 type I β turn.

(C) Covalent structure of a disulfide-linked conformationally constrained peptide designed to mimic structural and functional elements of ramoplanin's peptidoglycan intermediate capture motif.

(D) Part of the aliphatic region of the ^{1}H NMR spectrum of free peptide **16** (cyclic disulfide form, bottom trace), free Park's nucleotide (**11**, top trace), and a 1:1 mixture of the two (middle trace) depicting the chemical shift changes that occur upon binding.

(E) Plot of binding of peptide **16** to Park's nucleotide (**11**) as obtained by ^{1}H NMR titration. The solid circles denote the chemical shifts (δ) of the lactyl ether methyl protons (3a) of **11** as a function of the concentration of **16**.

types, potentially ameliorating chemical synthesis of the antibiotic and related analogs. Future structure/activity studies will help ascertain the requirements for both peptidoglycan capture and antimicrobial activity and will also shed light onto the interplay of intercomplex association/fibril formation with antibiotic activity.

Significance

Ramoplanin is an emerging clinical candidate antibiotic for treatment of VRE and MRSA infections. The antibiotic is in phase III trials for oral treatment of enterococcal infections. Ramoplanin is significantly

more potent than vancomycin for treatment of gram-positive bacterial infections. Here, we have further defined the essential structural elements of ramoplanin that confer antibiotic activity and high-affinity Lipid I/II binding. These results are significant because they suggest the existence of a minimalist pharmacophore and introduce the possibility of generating ramoplanin-derived peptide or peptidomimetic antibiotics for use against VRE, MRSA, and related pathogens.

Experimental Procedures

Methods and Materials

Mass spectra were recorded on Perspective BioSystems Voyager-DE RP MALDI-TOF or Hewlett-Packard ESI-MS spectrometers. Transmission electron micrographs were performed as previously described [16]. HPLC was performed on a Thermo-Separations TSP 3000 system using Phenomenex Jupiter or Vydac octadecyl silica columns. Fmoc-amino acids were purchased from Bachem. Routine one- and two-dimensional NMR spectroscopy was performed as previously described [16]. Measurement of dissociation constants was performed by NMR as previously reported [16]. Enduracidin was purchased from Sigma. Deuterated solvents were purchased from Aldrich and Cambridge Isotopes. UDP-MurNAc-L-Ala-γ-D-Glu-*meso*-Dap-D-Ala-D-Ala (**11**, Park's nucleotide), and UDP-MurNAc-L-Ala-γ-D-Glu-*meso*-Dap (**12**, UDP-MurNAc-tripeptide) were isolated from *Bacillus subtilis* ATCC 8037 according to the procedure of Holtje and coworkers [49]. 1-Phospho-MurNAc-L-Ala-γ-D-Glu-*meso*-Dap (**13**) was prepared according to the Van Heijenoort method [50]. L-Ala-γ-D-Glu-D-Lys-D-Ala-D-Ala (**9**) and MurNAc-L-Ala-γ-D-Gln (**15**) were purchased from Bachem. P^1-Citronellyl-P^2-MurNAc-L-Ala-γ-D-Glu-L-Lys-D-Ala-D-Ala pyrophosphate (**10**) and the related MurNAc pyrophosphate **14** were prepared as previously described [40]. Ramoplanin A2 aglycon (**2**) was synthesized by the method of Ciabatti [39]. Linearized Ramoplanin A2 (**6**) was produced by the procedure of Williams [48]. Minimal inhibitory concentrations were performed as previously reported [16].

Isothermal Titration Calorimetry

Isothermal titration calorimetry (ITC) experiments to measure interaction of Park's nucleotide (**11**) to guanidylated ramoplanin antibiotic derivative **3** were performed at 25°C using a Microcal MCS titration microcalorimeter equipped with a 250 μl injection syringe and a 400 rpm stirring rate. Both ramoplanin derivative **3** and PG analog **11** were dissolved in water and vacuum degassed before use. Compound **11** (20 × 10 μl injection of a 5.4 mM solution) was injected into an ITC cell containing ca. 1.3 ml of **3** (1 mM). Control experiments were performed under identical conditions by injection of **3** into water alone (to correct for heat of dilution effects), compound **11** into water, and the reverse experiment of titrating water into solutions of **3** or **11**. Titration data were processed using the software package Origin.

[Orn^4, Orn^{10}]-Diguanidylated Ramoplanin (3)

A dry nitrogen-flushed 50 ml round bottom flask was charged with Ramoplanin (200 mg, 0.0783 mmol, 1 eq), 1*H*-pyrazole-1-carboxamidine (458 mg, 1.57 mmol, 20 eq) and a teflon stirbar. The flask was sealed and diisopropylethylamine (372 mg, 1.57 mmol, 20 eq) in DMF (2 ml) was added by syringe. The solution was allowed to stir for 8 hr, then azeotropically evaporated with toluene under high vacuum three times and dried on high vacuum overnight. Excess starting material was removed by washing the solid with absolute ethanol (10 ml) with sonication, followed by filtration. The remaining solid was dissolved in HPLC Buffer A, purified by preparative reversed phase HPLC, and lyophilized to afford the title compound as a white solid (80.2 mg, 38.7% yield): MALDI TOF-MS calcd. 2638.15, actual 2639.5 (M + H); preparative HPLC conditions, Vydac C_{18} column (25 mm × 250 mm), mobile phase A = H_2O/ACN/TFA (80/20/0.1, v/v), mobile phase B = H_2O/ACN/TFA (10/90/0.1, v/v); analytical HPLC, Vydac C_{18} (4.5mm × 250mm) R_t: 35.05 min.

[Orn^4, Orn^{10}]-Diisovaleryl Ramoplanin (4)

A dry nitrogen-flushed 50 ml round bottom flask was charged with Ramoplanin (200 mg, 0.0783 mmol, 1.0 eq), a teflon stirbar, and sealed. Isovaleraldehyde (12 mg, 0.140 mmol, 1.8 eq, 15 μl) in DMF (2 ml) was added by syringe and the solution was allowed to stir for 2 hr. The solution was then treated with sodium cyanoborohydride (15 mg, 0.234 mmol, 3.0 eq) and stirred for an additional 2.5 hr. The reaction was then quenched with 0.1% aqueous TFA (25 ml), purified by preparative reversed phase HPLC, and lyophilized to give **4** as a white solid (31.0 mg, 15%). MALDI TOF-MS calcd. 2694.33, actual 2696.0 (M + H); preparative HPLC conditions, Vydac C_{18} column (25 mm × 250 mm), mobile phase A = H_2O/ACN/TFA (80/20/0.1, v/v), mobile phase B = H_2O/ACN/TFA (20/80/0.1, v/v); analytical HPLC: Vydac C_{18} (4.5mm × 250mm) R_t: 38.98 min.

[Orn^4, Orn^{10}]-Diacetylated Ramoplanin (5)

A dry nitrogen-flushed 50 ml round bottom flask was charged with Ramoplanin (100 mg, 0.0392 mmol, 1.0 eq), a teflon stirbar, and sealed. Acetonitrile (6 ml) and DMF (5.5 ml) were added by syringe, and the stirred solution was chilled on an ice bath. Acetic anhydride (8 mg, 0.0783 mmol, 2.0 eq) and a catalytic amount of pyridine (0.1 mol %) were added, the solution was stirred at 0°C for 1 hr and then allowed to warm to room temperature and stir for 3 hr. The solution was then diluted with aqueous TFA (10 ml, 0.1% v/v) and purified by HPLC to afford **5** as a white solid (11.4 mg, 11%): MALDI TOF-MS calcd. 2638.14, actual 2639.3 (M + H); preparative HPLC conditions, Vydac C_{18} column (25 mm × 250 mm), mobile phase A = H_2O/ACN/TFA (80/20/0.1, v/v), mobile phase B = H_2O/ACN/TFA (20/80/0.1, v/v); analytical HPLC, Vydac C_{18} (4.5 mm × 250 mm) R_t: 36.09 min.

N^{α}-Octanoyl-Asn-Asn-cyclo[Cys-D-Orn-Phe-*allo*Thr-D-Hpg-D-*allo*Thr-Hpg-Cys]-D-Orn-NH_2 (16)

The linear peptide was prepared by solid-phase peptide synthesis on an Applied Biosystems 433 peptide synthesizer on a 0.25 mmol scale using Fmoc-protected amino acids and HBTU/HOBt activation. No side chain protection was employed for *allo*-Thr and Hpg residues. Following assembly of the linear peptide sequence, the N terminus was acylated with octanoic acid (Acros Chemicals). The peptide resin was cleaved with TFA/H_2O/EDT (94:2.5:2.5:1 v/v) for 3 hr at room temperature according to standard methods, and the crude peptide was precipitated with cold Et_2O (−40°C). Intramolecular cyclization to the disulfide was accomplished by stirring a ca. 1 mM solution of the crude peptide in 20% DMSO/H_2O for four days in a 250 ml round bottom flask exposed to air. The crude cyclic peptide was purified to homogeneity by reversed-phase HPLC (conditions: Phenomenex Jupiter C_4 column (5μ, 300 Å, 250 × 21.2 mm); mobile phase A, H_2O/heptafluoroisobutyric acid (99.9/0.1, v/v), mobile phase B, ACN/H_2O/heptafluoroisobutyric acid (89.9/10/0.1, v/v/v). Fractions containing pure cyclic peptide were identified by MS, combined, and lyophilized to yield pure **16** (52 mg) as a white powder: HR-MS (ESI) m/z: calcd. 1339.58151, actual 1339.5803 (M + H); ^{1}H NMR (D_2O) δ 0.713 (t, *J* = 7.0 Hz, octanoic acid CH_3), 0.967 (d, *J* = 6.5 Hz, Thr^8 HCγ), 0.989-1.113 (m, octanoic acid HC γ, δ, ϵ, ξ, Orn^4 HCγ, Orn^4 HCβ, Thr^5 HCγ), 1.308 (m, Orn^4 HCβ), 1.440 (m, Orn^{10} HCγ), 1.574 (m, Orn^4 HCβ), 1.767 (m, Orn^4 HCβ), 2.011 (m, Orn^4, HCδ), 2.105 (d, *J* = 5.5 Hz, octanoic acid HCα), 2.622 (m, Asn^1 HCβ), 2.776 (m, Orn^4 HCδ), 2.864-2.887 (m, Orn^4 HCδ, Cys^9 HCβ), 2.976 (m, Cys^2 HCβ), 3.072 (m, Cys^9 HCβ), 3.150 (m, Cys^2 HCβ), 3.909 (m, Thr^8 HCα), 4.122 (m, Thr^5 HCβ), 4.221-4.237 (m, Orn^{10} HCα, Thr^8 HCβ), 4.562 (m, Orn^4 HCα), 4.719-4.764 (m, Asn^1 HCα), 5.233 (s, Hpg^6 HCα), 5.277 (s, Orn^{10} HCα), 5.385 (s, Hpg^3 HCα), 5,520 (s, Hpg^7 HCα), 6.737 (d, *J* = 8.5 Hz Hpg^6 aromatic c,e), 6.769 (d, *J* = 8.5 Hz, Hpg^3 aromatic c,e), 6.799 (d, *J* = 8.5 Hz, Hpg^7 aromatic c,e), 7.088 (d, *J* = 8.0 Hz Hpg^6 aromatic b,f), 7.129 (d, *J* = 8.5 Hz, Hpg^3 aromatic b,f), 7.182 (d, *J* = 8.5 Hz, Hpg^7 aromatic b,f) ppm; ^{13}C NMR (D_2O) δ 16.150, 21.565, 21.796, 24.734, 26.045, 28.000, 30.161, 30.695, 30.853, 30.950, 33.718, 38.210, 38.878, 41.415, 41.488, 41.561, 53.131, 55.390, 55.815, 56.264, 56.519, 59.238, 59.809, 60.695, 62.407, 62.832, 69.607, 118.450, 118.595, 118.644, 118.862, 129.364, 130.214, 130.566, 131.538, 131.756, 131.890, 132.157, 132.388, 173.655, 173.934, 174.262, 174.407, 174.588, 174.942, 175.111, 175.281, 175.415, 176.192, 176.823, 178.268, 179.846 ppm.

Acknowledgments

We gratefully acknowledge Hellina Tadesse for isolating Park's nucleotide. This work was generously supported by grants from the McCabe Foundation (to D.G.M.), the American Cancer Society (RPG-99-31-02-CCE, D.G.M.), and by the National Institutes of Health (AI46611, D.G.M.; DK39806, A.J.W.; HL30954, J.W.W.) J.K.K. is the recipient of an NIH NRSA fellowship (GM20206).

Received: May 22, 2002
Revised: July 16, 2002
Accepted: July 16, 2002

References

1. Swartz, M.N. (1994). Hospital-acquired infections: Diseases with increasingly limited therapies. Proc. Natl. Acad. Sci. USA *91*, 2420–2427.
2. Gold, H.S., and Moellering, R.C. (1996). Antimicrobial-drug resistance. N. Engl. J. Med. *335*, 1445–1452.
3. Malabarba, A. (1996). New approaches to the treatment of vancomycin-resistant bacterial infections. Expert Opin. Ther. Pat. *6*, 627–644.
4. O'Hare, M.D., Ghosh, G., Felmingham, D., and Grueneberg, R.N. (1990). In vitro studies with ramoplanin (MDL 62,198): a novel lipoglycopeptide antimicrobial. J. Antimicrob. Chemother. *25*, 217–220.
5. O'Hare, M.D., Felmingham, D., and Gruneberg, R.N. (1988). The in vitro activity of ramoplanin (A-16686/MDL 62,198), vancomycin and teicoplanin against methicillin-susceptible and methicillin-resistant Staphylococcus spp. Drugs Exp. Clin. Res. *14*, 617–619.
6. Maple, P.A.C., Hamilton-Miller, J.M.T., and Brumfitt, W. (1989). Comparative in vitro activity of vancomycin, teicoplanin, ramoplanin (formerly A16686), paldimycin, DuP 721 and DuP 105 against methicillin and gentamicin resistant *Staphylococcus aureus*. J. Antimicrob. Chemother. *23*, 517–525.
7. Brumfitt, W., Maple, P.A.C., and Hamilton-Miller, J.M.T. (1990). Ramoplanin versus methicillin-resistant Staphylococcus aureus: in vitro experience. Drugs Exp. Clin. Res. *16*, 377–383.
8. Collins, L.A., Eliopoulos, G.M., Wennersten, C.B., Ferraro, M.J., and Moellering, R.C., Jr. (1993). In vitro activity of ramoplanin against vancomycin-resistant gram-positive organisms. Antimicrob. Agents Chemother. *37*, 1364–1366.
9. Johnson, C.C., Taylor, S., Pitsakis, P., May, P., and Levison, M.E. (1992). Bactericidal activity of ramoplanin against antibiotic-resistant enterococci. Antimicrob. Agents Chemother. *36*, 2342–2345.
10. Ciabatti, R., Kettenring, J.K., Winters, G., Tuan, G., Zerilli, L., and Cavalleri, B. (1989). Ramoplanin (A-16686), a new glycolipodepsipeptide antibiotic. III. Structure elucidation. J. Antibiot. (Tokyo) *42*, 254–267.
11. Cavalleri, B., Pagani, H., Volpe, G., Selva, E., and Parenti, F. (1989). A-16686, a new antibiotic from Actinoplanes. I. Fermentation, isolation and preliminary physicochemical characteristics. J. Antibiot. (Tokyo) *37*, 309–317.
12. Pallanza, R., Berti, M., Scotti, R., Randishi, E., and Arioli, V. (1984). A-16686, a new antibiotic from Actinoplanes. II. Biological properties. J. Antibiot. (Tokyo) *37*, 318–324.
13. Parenti, F., Ciabatti, R., Cavalleri, B., and Kettenring, J. (1990). Ramoplanin: a review of its discovery and its chemistry. Drugs Exp. Clin. Res. *16*, 451–455.
14. Reynolds, P.E., and Somner, E.A. (1990). Comparison of the mechanism of action of glycopeptide and lipoglycodepsipeptide antibiotics. Drugs Exp. Clin. Res. *16*, 385–389.
15. Somner, E.A., and Reynolds, P.E. (1990). Inhibition of peptidoglycan biosynthesis by ramoplanin. Antimicrob. Agents Chemother. *34*, 413–419.
16. Cudic, P., Kranz, J., Behenna, D.C., Kruger, R.G., Tadesse, H., Wand, A.J., Veklich, Y.I., Weisel, J.W., and McCafferty, D.G. (2002). Complexation of peptidoglycan intermediates by the lipoglycodepsipeptide antibiotic ramoplanin: Minimal structural requirements for intermolecular complexation and fibril formation. Proc. Natl. Acad. Sci. USA *99*, 7384–7389.
17. Lo, M.C., Men, H., Branstrom, A., Helm, J., Yao, N., Goldman, R., and Walker, S. (2000). A new mechanism of action proposed for ramoplanin. J. Am. Chem. Soc. *122*, 3540–3541.
18. Iwasaki, H., Horii, S., Asai, M., Mizuno, K., Ueyanagi, J., and Miyake, A. (1973). Enduracidin, a new antibiotic. VIII. Structure of enduracidins A and B. Chem. Pharm. Bull. (Tokyo) *21*, 1184–1191.
19. Higashide, E., Hatano, K., Shibata, M., and Nakazawa, K. (1968). Enduracidin, a new antibiotic. I. *Streptomyces fungicidicus* No. B 5477, an enduracidin producing organism. J. Antibiot. (Tokyo) *21*, 126–137.
20. Tsuchiya, K., and Takeuchi, Y. (1968). Enduracidin, an inhibitor of cell wall synthesis. J. Antibiot. (Tokyo) *21*, 426–428.
21. Brown, W.E., Seinerova, V., Chan, W.M., Laskin, A.I., Linnett, P., and Strominger, J.L. (1974). Inhibition of cell wall synthesis by the antibiotics diumycin and janiemycin. Ann. N Y Acad. Sci. *235*, 399–405.
22. Linnett, P.E., and Strominger, J.L. (1973). Additional antibiotic inhibitors of peptidoglycan synthesis. Antimicrob. Agents Chemother. *4*, 231–236.
23. Meyers, E., Weisenborn, F.L., Pansy, F.E., Slusarchyk, D.S., Von Saltza, M.H., Rathnum, M.L., and Parker, W.L. (1970). Janiemycin, a new peptide antibiotic. J. Antibiot. (Tokyo) *23*, 502–507.
24. Brotz, H., Bierbaum, G., Reynolds, P.E., and Sahl, H.G. (1997). The lantibiotic mersacidin inhibits peptidoglycan biosynthesis at the level of transglycosylation. Eur. J. Biochem. *246*, 193–199.
25. Brotz, H., Bierbaum, G., Leopold, K., Reynolds, P.E., and Sahl, H.G. (1998). The lantibiotic mersacidin inhibits peptidoglycan biosynthesis by targeting Lipid II. Antimicrob. Agents Chemother. *42*, 154–160.
26. Prasch, T., Nauman, T., Markert, R.L., Sattler, M., Schubert, M., Schaal., S., Bauch, M., Kogler, H., and Greisinger, C. (1997). Constitution and solution conformation of the antibiotic mersacidin determined by NMR and molecular dynamics. Eur. J. Biochem. *244*, 501–512.
27. Schneider, T.R., Karcher, J., Pohl, E., Lubini, P., and Sheldrick, G.M. (2000). Ab initio structure determination of the lantibiotic mersacidin. Acta Crystallogr. D Biol. Crystallogr. *D56*, 705–713.
28. Zimmermann, N., and Jung, G. (1997). The three-dimensional solution structure of the lantibiotic murein-biosynthesis-inhibitor actagardine determined by NMR. Eur. J. Biochem. *246*, 809–819.
29. McCafferty, D.G., Cudic, P., Yu, M.K., Behenna, D.C., and Kruger, R. (1999). Synergy and duality in peptide antibiotic mechanism. Curr. Opin. Chem. Biol. *3*, 672–680.
30. Bierbaum, G., Brotz, H., and Sahl, H.-G. (1997). Lanthionine-containing antibiotic peptides (lantibiotics): features, functions and perspectives. Biospektrum *2*, 51–55.
31. Bierbaum, G. (1999). Antibiotic peptides: lantibiotics. J. Chemother. *8*, 204–209.
32. Guder, A., Wiedemann, I., and Sahl, H.-G. (2000). Posttranslationally modified bacteriocins - the lantibiotics. Biopolymers *55*, 62–73.
33. Men, H., Park, P., Ge, M., and Walker, S. (1998). Substrate synthesis and activity assay for MurG. J. Am. Chem. Soc. *120*, 2484–2485.
34. Ciabatti, R., and Cavalleri, B. (1992). Hydrogenated derivatives of antibiotic A/16686, Gruppo Lepetit, S.P.A.: United States 5,108,988.
35. Kurz, M., and Guba, W. (1996). 3D Structure of ramoplanin: A potent inhibitor of bacterial cell wall synthesis. Biochemistry *35*, 12570–12575.
36. Gerhard, U., Mackay, J.P., Maplestone, R.A., and Williams, D.H. (1993). The role of the sugar and chlorine substituents in the dimerization of vancomycin antibiotics. J. Am. Chem. Soc. *115*, 232–237.
37. Harris, C.M., Kannan, R., Kopecka, H., and Harris, T.M. (1985). The role of the chlorine substituents in the antibiotic vancomycin: Preparation and characterization of monodechlorovancomycin and didechlorovancomycin. J. Am. Chem. Soc. *107*, 6652–6658.
38. Ciabatti, R., and Cavalleri, B. (1989). Aglycons of A16686 antibi-

otics. In Eur. Pat. Appl. (Gruppo Lepetit S.P.A., Italy), 21 p., Ep. 337203.
39. Ciabatti, R., and Cavalleri, B. (1996). Aglycons of A/16686 antibiotics, Gruppo Lepetit, S.P.A.: United States 5,491,128.
40. Cudic, P., Behenna, D.C., Yu, M.K., Kruger, R., Szewczuk, L., and McCafferty, D.G. (2001). Synthesis of P^1-citronellyl-P^2-α-D-pyranosyl pyrophosphates as potential substrates for the *E. coli* undecaprenyl-pyrophosphoryl-*N*-acetylglucoseaminyl transferase MurG. Bioorg. Med. Chem. Lett. *11*, 3107–3110.
41. Park, J.T. (1952). Uridine-5′-pyrophosphate derivatives. J. Biol. Chem. *194*, 877–904.
42. Wyss, D.F., and Wagner, G. (1996). The structural role of sugars in glycoproteins. Curr. Opin. Biotechnol. *7*, 409–416.
43. Farnet, C.M., Zazopoulos, E., and Staffa, A. (2002). Ramoplanin biosynthesis genes and enzymes of Actinoplanes. In PCT Int. Appl. (Ecopia Biosciences Inc., Can.), 212 p., WO 0231155.
44. Fujisawa, H., Ise, J., Okada, Y., Mori, A., Aoki, K., and Shimamoto, T. (1971). Behavior of enramycin in aqueous solution. Takeda Kenkyusho Ho *30*, 336–343.
45. Jiang, W., Wanner, J., Lee, R.J., Bounaud, P.-Y., and Boger, D.L. (2002). Total synthesis of the ramoplanin A2 and ramoplanose aglycon. J. Am. Chem. Soc. *124*, 5288–5290.
46. Cooper, A. (1997). Micro-calorimetry of protein-protein interactions. In Methods in Molecular Biology, Volume 88: Protein Targeting Protocols, R.A. Clegg, ed. (Totowa, N. J.: Humana Press), pp. 11–23.
47. Cooper, A., and McAuley-Hecht, K.E. (1993). Microcalorimetry and the molecular recognition of peptides and proteins. Phil. Trans. R. Soc. Lond. A *345*, 23–35.
48. Maplestone, R.A., Cox, J.P.L., and Williams, D.H. (1993). Retention of native-like structure in an acyclic counterpart of a beta-sheet antibiotic. FEBS Lett. *326*, 95–100.
49. Kohlrausch, U., and Holtje, J.V. (1991). One-step purification procedure for UDP-*N*-acetylmuramyl-peptide murein precursors from *Bacillus cereus*. FEMS Microbiol. Lett. *78*, 253–258.
50. Auger, G., Crouvoisier, M., Caroff, M., van Heijenoort, J., and Blanot, D. (1997). Synthesis of an analogue of the lipoglycopeptide membrane intermediate I of peptidoglycan biosynthesis. Letters in Peptide Science: LIPS *4*, 371–376.
51. Hori, M., Iwasaki, H., Horii, S., Yoshida, I., and Hongo, T. (1973). Enduracidin, a new antibiotic. VII. Primary structure of the peptide moiety. Chem. Pharm. Bull. (Tokyo) *21*, 1175–1183.